ISSN 1068-798X, Russian Engineering Research, 2009, Vol. 29, No. 12, pp. 1248–1254. © Allerton Press, Inc., 2009.
Original Russian Text © S.I. Petrushin, A.V. Proskokov, 2009, published in Vestnik Mashinostroeniya, 2009, No. 12, pp. 58–64.

Theory of Constrained Motion of Materials: Chip Formation with a Single Conditional Shear Surface

S. I. Petrushin[a] and A. V. Proskokov[b]

[a]*Tomsk Polytechnic University*

[b]*Yurginsk Technological Institute, a Branch of Tomsk Polytechnic University*

Abstract—Orthogonal constrained cutting is considered. The initial direction of chip flow for a curvilinear blade with an inclined cutting face is analyzed, in static coordinates.

DOI: 10.3103/S1068798X09120119

Most research on chip formation is based on free cutting with a single shear plane (the approach proposed by I.A. Time). No account is taken of the two-dimensional blade geometry nor of the three-dimensional character of the deformation source in the cut layer. It is assumed that the transformation of the cut layer into chip is confined to a very narrow zone adjacent to the shear plane. By contrast, constrained cutting is characterized by a conditional three-dimensional shear surface, which is analogous to the shear plane.

In the analysis of chip formation for constrained cutting, a cutter formed by two rectilinear cutting edges (a sharp tip) was considered in [1, 2]. In this approach, it is assumed that the conditional shear planes emerge from these edges and are inclined at different shear angles to the cutting-speed vector. For a curvilinear cutting blade, this approach is inapplicable, since the conditional shear surface will have a different shear angle at each point of the cutting edge, which results in indeterminacy of its shape.

We should distinguish between orthogonal and oblique constrained cutting. Orthogonal constrained cutting is a process in which, regardless of the shape of the cutting edge, the plane front surface of the blade is perpendicular to the cutting-speed vector v for static coordinates or to the velocity vector v_e of the resultant cutting motion for kinematic coordinates.

In the dynamic coordinate system $x_d y_d z_d$, orthogonal constrained cutting by a blade with a plane front surface and a curvilinear cutting edge is shown in Fig. 1 [3]; chip formation is mainly due to the curvilinear cutting edge. The following assumptions are made here:

(1) the transformation of the cut layer *ABC* to chip is confined to a narrow zone adjacent to the conditional shear surface *ABD*;

(2) chip moves along the front surface as a single body, in the direction determined by the initial departure angle η;

(3) in the chip-root cross sections parallel to the secant departure plane P_c, free orthogonal cutting occurs for point i of the cutting edge with definite values of the shrinkage coefficient ζ_{ai} and shear angle φ_i;

(4) the shape and size of the chip cross section are determined by the projection of the conditional shear surface onto the plane $x_d O z_d$. (Deformation of the layer at the cutting edge is disregarded.)

The conditional shear surface has a complex curvilinear three-dimensional form (Fig. 1), bounded below by the working section *AB* of the cutting edge and above by the transition line *DB* between the external chip surface and the cutting surface corresponding to the previous position of the edge, as well as the line *AD* along which the conditional shear surface reaches the machined surface.

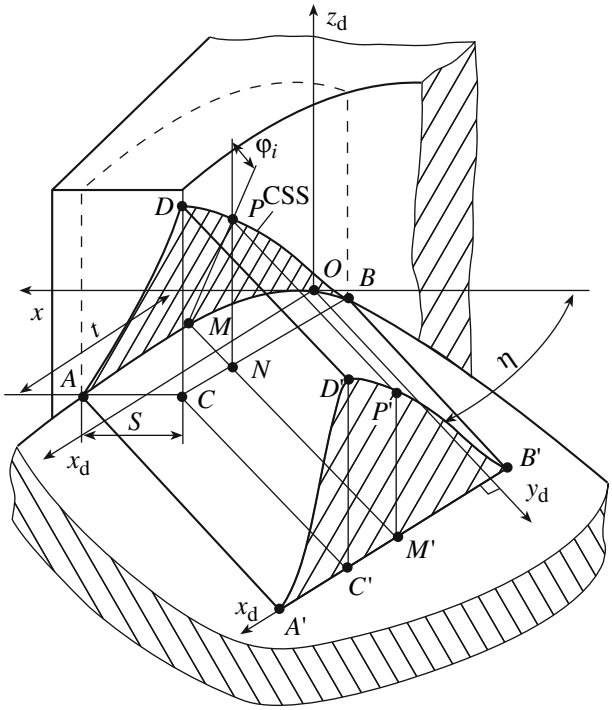

Fig. 1. Orthogonal constrained cutting: CSS, conditional shear surface.

Consider cross section i of the chip root at point M. The thickness a' of the cut layer in the direction of chip departure is determined by the segment MN and calculated from Eq. (24) in [3]. If the dynamic front angle $\gamma_d = 0$, then $\tan\varphi_i = 1/\zeta_{ai} = a_i'/a_{c_i}$, where a_i' and a_{c_i} are the thickness of the cut layer and the chip in the direction of departure, respectively.

Then, the height of the conditional shear surface in this cross section (NP in Fig. 1) or, equivalently, the chip thickness ($M'P'$) may be found from the formula

$$a_{c_i} = a_i'/\tan\varphi_i. \tag{1}$$

If $\gamma_d \neq 0$, while the dynamic inclination of the blade $\lambda_d = 0$, the process may be regarded as orthogonal constrained cutting. The chip thickness in cross section i is then

$$a_{c_i} = a_i\frac{\cos(\varphi_i - \gamma_d)}{\sin\varphi_i}. \tag{2}$$

The variation in the shear angle in the cross sections of the chip root parallel to its direction of departure remains to be determined. On the one hand, in free cutting, φ_i increases with decrease in chip thickness a_i, as established experimentally [4]. On the other, φ_i increases with increase in a_i/b_i during constrained cutting [2]. Probably, the difference between the plane and three-dimensional stress–strain state of the cut layer plays an important role in both cases. Therefore, we may assume that the shear angle φ_i is the same for any point on the working section of the curvilinear cutting blade for constrained cutting in the direction of chip departure over the front surface [5]. Then Eqs. (1) and (2) take the form

$$a_{c_i} = \frac{a_i}{\tan\varphi_{cu}}; \quad a_{c_i} = a_i\frac{\cos(\varphi_{cu} - \gamma_d)}{\sin\varphi_{cu}}.$$

We now construct the conditional shear surface for an arbitrary cutting plane in the case of oblique constrained cutting, which is widely used in metalwork with chip removal and is poorly suited to analytical description since $\lambda_d \neq 0$, with additional deviation of the direction of chip departure.

A curvilinear blade whose plane front surface is inclined by γ_x and γ_y relative to the static coordinates is shown in Fig. 2. The conditional shear surface is also plotted in Fig. 2, in the form of the closed contour ABD. (The blank and chip are not shown.) For specified t and S, the cross section $A'BC'$ of the cut layer corresponds to the projection ABC on the front surface of the blade. We now find the equation of the line DB, which forms the upper bound on the conditional shear surface; its lower bound is the section AB of the curvilinear cutting edge.

Adopting the machine-tool coordinate system, we eliminate the parameter t from Eq. (3) in [3]

$$\begin{cases} y = f(x); \\ z = \psi(x). \end{cases} \tag{3}$$

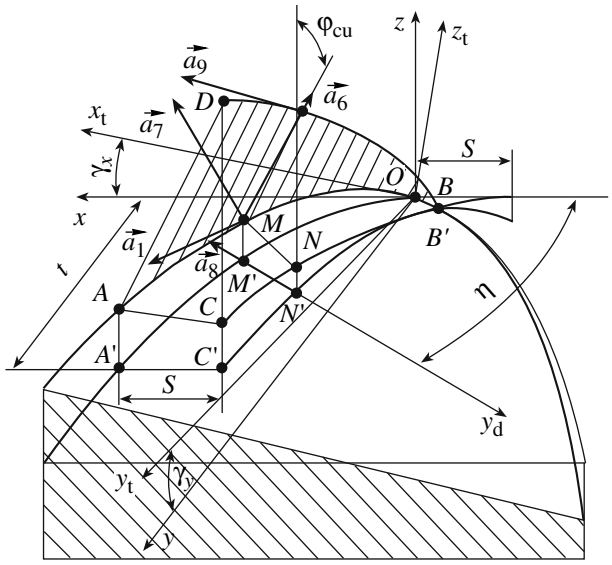

Fig. 2. Conditional shear surface in oblique constrained cutting.

The equation of the cutting edge's previous position (in terms of the supply S) takes the form

$$\begin{cases} y = f(x + S); \\ z = \psi(x + S). \end{cases} \tag{4}$$

Then, for the tangent to the cutting edge at arbitrary point M (Fig. 2), we rewrite Eq. (2) from [3]

$$\vec{a}_1 = \vec{i} + y_M'\vec{j} + z_M'\vec{k}, \tag{5}$$

where y_M' and z_M' are derivatives of Eq. (3) with respect to x at the given point.

On the basis of the assumptions adopted, the unit directional vector $\vec{a}_6$, determining the direction of the generatrix of the conditional shear surface as a linear surface takes the form

$$\vec{a}_6 = -\sin\varphi_{cu}\cos\eta\cdot\vec{i} + \sin\varphi_{cu}\sin\eta\cdot\vec{j} + \cos\varphi_{cu}\cdot\vec{k}. \tag{6}$$

The directional vector of the normal to the conditional shear surface at point M is equal to the vector product $\vec{a}_7 = \vec{a}_1 \times \vec{a}_6$. Taking account of Eqs. (5) and (6)

$$\vec{a}_7 = [(\cos\varphi_{cu}\cdot y_M' - \sin\varphi_{cu}\sin\eta\cdot z_M')\vec{i} - (\cos\varphi_{cu} + \sin\varphi_{cu}\cos\eta\cdot z_M')\vec{j} + \sin\varphi_{cu}(\sin\eta + \cos\eta\cdot y_M')\vec{k}]\sin\mu, \tag{7}$$

where μ is the angle between vectors $\vec{a}_1$ and $\vec{a}_6$.

The directional vector normal to the cutting surface formed by the previous position of the cutting edge leaving point N' (Fig. 2) is found from the formula

$$\vec{a}_8 = \frac{y'_{N'}}{\sqrt{1+y'^2_{N'}}}\vec{i} - \frac{1}{\sqrt{1+y'^2_{N'}}}\vec{j}, \tag{8}$$

where $y'_{N'}$ is the derivative of the first relation in Eq. (4) at the point N'.

Then the directional vector of the tangent to line OA is determined by the vector product $\vec{a}_9 = \vec{a}_7 \times \vec{a}_8$. After appropriate transformations, we obtain

$$\begin{aligned}\vec{a}_9 &= \frac{\sin\varphi_{cu}(\sin\eta + \cos\eta \cdot y'_M)}{\sqrt{1+y'^2_{N'}}}\vec{i} \\ &+ \frac{\sin\varphi_{cu} \cdot y'_{N'}(\sin\eta + \cos\eta \cdot y'_M)}{\sqrt{1+y'^2_{N'}}}\vec{j} \\ &+ \frac{\cos\varphi_{cu}(y'_{N'} - y'_M) + \sin\varphi_{cu} \cdot z'_M(\sin\eta + \cos\eta \cdot y'_{N'})}{\sqrt{1+y'^2_{N'}}}\vec{k}.\end{aligned} \tag{9}$$

The coefficients preceding the unit vectors in Eq. (9) are the directional cosines of the tangent to line DB at the current point. Therefore, the projection of line DB onto the xOz plane may be determined from its derivative, which is the directional-cosine ratio $\cos\alpha_z/\cos\alpha_x$ or

$$\begin{aligned}DB'_{xOz} &= \frac{y'_{N'} - y'_M + \tan\varphi_{cu} \cdot z'_M(\sin\eta + \cos\eta \cdot y'_{N'})}{\tan\varphi_{cu}(\sin\eta + \cos\eta \cdot y'_M)}\end{aligned} \tag{10}$$

Integrating Eq. (10), we obtain

$$\begin{aligned}DB_{xOz} &= \frac{1}{\tan\varphi_{cu}} \\ &\times \int \frac{y'_{N'} - y'_M + \tan\varphi_{cu} \cdot z'_M(\sin\eta + \cos\eta \cdot y'_{N'})}{\sin\eta + \cos\eta \cdot y'_M}\mathrm{d}x + C_1,\end{aligned} \tag{11}$$

where the constant C_1 is determined from the condition that $z_B = DB_{xOz}$ at point B.

To determine the projection of line DB onto the yOz plane, we must rewrite all the expressions so that they depend on y. Then Eqs. (3) and (4) take the form

$$\begin{cases} x = \varphi(y); \\ z = \zeta(y); \end{cases} \tag{12}$$

$$\begin{cases} x = \varphi(y) - S; \\ z = \zeta(y). \end{cases} \tag{13}$$

Proceeding analogously, we write Eqs. (5) and (7)–(9) in the form

$$\begin{aligned}\vec{a}_1 &= x'_M\vec{i} + \vec{j} + z'_M\vec{k}; \\ \vec{a}_7 &= [(\cos\varphi_{cu} - \sin\varphi_{cu}\sin\eta \cdot z'_M)\vec{i} \\ &- (x'_M\cos\varphi_{cu} + z'_M\sin\varphi_{cu}\cos\eta)\vec{j} \\ &+ \sin\varphi_{cu}(x'_M\sin\eta + \cos\eta)\vec{k}]\sin\mu; \\ \vec{a}_8 &= \frac{1}{\sqrt{1+x'^2_{N'}}}\vec{i} - \frac{x'_{N'}}{\sqrt{1+x'^2_{N'}}}\vec{j}; \\ \vec{a}_9 &= \frac{x'_{N'}\sin\varphi_{cu}(x'_M\sin\eta + \cos\eta)}{\sqrt{1+x'^2_{N'}}}\vec{i} \\ &+ \frac{\sin\varphi_{cu}(x'_M\sin\eta + \cos\eta)}{\sqrt{1+x'^2_{N'}}}\vec{j} \\ &+ \frac{\cos\varphi_{cu}(x'_M - x'_{N'}) + z'_M\sin\varphi_{cu}(x'_{N'}\sin\eta + \cos\eta)}{\sqrt{1+x'^2_{N'}}}\vec{k},\end{aligned}$$

where x'_M and z'_M are the derivatives of the functions in Eq. (12) with respect to y; $x_{N'}$ is the abscissa of point N' (Fig. 2).

Hence, we obtain an expression for the derivative of the projection of line DB onto the yOz plane

$$\begin{aligned}DB'_{yOz} &= \frac{\cos\alpha_z}{\cos\alpha_y} \\ &= \frac{x'_M - x'_{N'} + z'_M\tan\varphi_{cu}(\cos\eta + x'_{N'}\sin\eta)}{\tan\varphi_{cu}(x'_M\sin\eta + \cos\eta)},\end{aligned}$$

Integration yields

$$\begin{aligned}DB_{yOz} &= \frac{1}{\tan\varphi_{cu}} \\ &\times \int \frac{x'_M - x'_{N'} + z'_M\tan\varphi_{cu}(\cos\eta + x'_{N'}\sin\eta)}{x'_M\sin\eta + \cos\eta}\mathrm{d}y + C_2,\end{aligned} \tag{14}$$

where C_2 is found from the condition that $z_B = DB_{yOz}$ at point B.

When $\gamma_x = \gamma_y = 0$ (in other words, for orthogonal constrained cutting), Eqs. (11) and (14) take the form

$$DB_{xOz} = \frac{1}{\tan\varphi_{cu}\cos\eta}\int \frac{y'_{N'} - y'_M}{\tan\eta + y'_M}\mathrm{d}x + C_3; \tag{15}$$

$$DB_{yOz} = \frac{1}{\tan\varphi_{cu}\cos\eta}\int \frac{x'_M - x'_{N'}}{\tan\eta + x'_M}\mathrm{d}y + C_4, \tag{16}$$

where the constants C_3 and C_4 are determined from the condition that $DB_{xOz} = DB_{yOz} = 0$ at point B.

The formulas obtained for the upper bound on the conditional shear surface include partial derivatives (at point

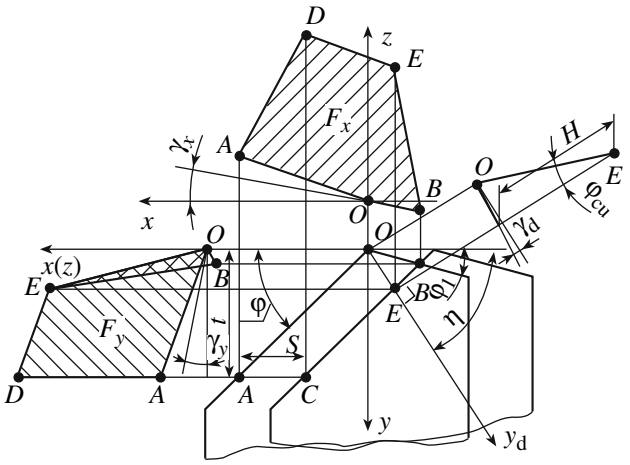

Fig. 3. Conditional shear surface for a sharp tip.

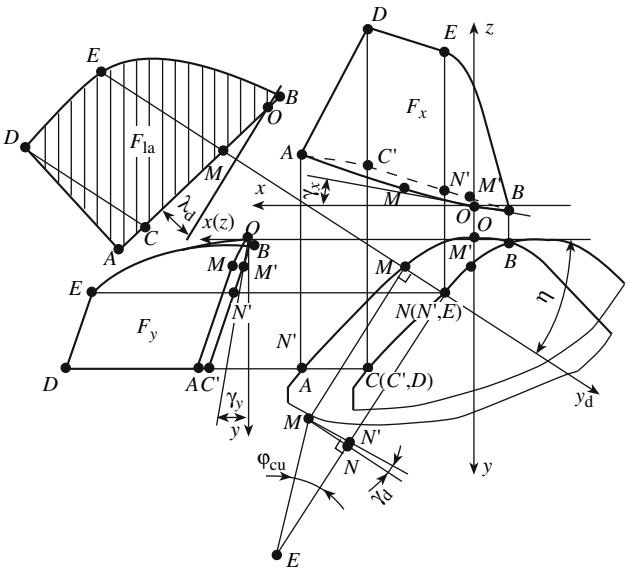

Fig. 4. Conditional shear surface for a rounded tip.

N') of functions describing the previous position of the cutting edge at the basic plane. The coordinates of point N' are determined by the method in [3].

We now investigate particular cases of the construction of the conditional shear surface in constrained oblique cutting, on the assumption of a cutting blade with a sharp point and standard geometry (a rounded tip). We also assume that φ = const in the direction of chip departure for any point within the working section of the cutting edge.

A sharp blade with a plane front surface is shown in Fig. 3. The position of the front surface is specified by the frontal and profile angles γ_x and γ_y.

In these conditions, the equation of the primary cutting edge is

$$\begin{cases} y = \tan\varphi \cdot x; \\ z = \left(\dfrac{\tan\gamma_x}{\cos\gamma_y} + \tan\varphi\tan\gamma_y\right)x; \end{cases} \tag{17}$$

the equation of the preceding position of the primary cutting edge is

$$\begin{cases} y = \tan\varphi(x + S); \\ z = \left(\dfrac{\tan\gamma_x}{\cos\gamma_y} + \tan\varphi\tan\gamma_y\right)(x + S); \end{cases} \tag{18}$$

and the equation of the auxiliary cutting edge is

$$\begin{cases} y = -\tan\varphi_1 \cdot x; \\ z = \left(\dfrac{\tan\gamma_x}{\cos\gamma_y} - \tan\varphi_1\tan\gamma_y\right)x. \end{cases}$$

Since the cutting edge is specified by a discontinuous line in this case, the conditional shear surface is constructed in sections. When $x \geq 0$, we substitute the corresponding derivatives from Eqs. (17) and (18) into Eqs. (11) and (14), to obtain the following expressions for the upper bound of the conditional shear surface

$$DE_{xOz} = \left(\frac{\tan\gamma_x}{\cos\gamma_y} + \tan\varphi\tan\gamma_y\right)x + H;$$

$$DE_{yOz} = \left(\frac{\tan\gamma_x}{\cos\gamma_y\tan\varphi} + \tan\gamma_y\right)y + H,$$

where

$$H = \frac{S\sin\varphi}{\tan\varphi_{cu}\sin(\varphi + \eta)}$$

is the height of the conditional shear surface.

The lower bound on the conditional shear surface in this section is specified by the projections of the primary cutting edge onto the coordinate planes.

In the section $0 > x > x_B$, the upper bound on the conditional shear surface has the point of discontinuity E, whose position is determined by the coordinates

$$X_E = -\frac{S\sin\varphi\cos\eta}{\sin(\varphi + \eta)};$$

$$Y_E = \frac{S\sin\varphi\cos\eta}{\sin(\varphi + \eta)}.$$

On the basis of the results, the projections of the conditional shear surfaces F_x and F_y onto planes zOx and zOy are plotted in Fig. 4. The distinguishing feature of F_x is the addition of a triangle with the base S, while F_y contains a latent surface F_{la}, which is shaded in Fig. 4.

Often, the cutting edge (or part of it) takes the form of a surface. We now describe the conditional shear surface in that case for a ground tool, when the tip rounding is specified in the machine-tool coordinate system (Fig. 4). Suppose that the working part of the cutting edge consists of a

linear primary cutting edge *AM* and a transition segment *MB*, which forms part of a circle (radius *r*) in the coordinates *xyz*. This corresponds to the auxiliary cutting edge.

The plane front surface of the blade is inclined at the frontal angle γ_x and the profile angle γ_y with respect to the static basic plane. Solving the first two relations in Eq. (16) and the equation of the front surface in the tool coordinate system $z_t = 0$, according to Eq. (5) in [3], we obtain the following equations:

—the projection of the primary cutting edge onto coordinate plane *xOz*

$$Z_x = \left(\frac{\tan\gamma_x}{\cos\gamma_y} + \tan\varphi\tan\gamma_y\right)x + r\tan\gamma_y(1 - \cos\varphi - \tan\varphi\sin\varphi); \quad (19)$$

—the projection of the primary cutting edge onto coordinate plane *yOz*

$$Z_y = \left(\frac{\tan\gamma_x}{\tan\varphi\cos\gamma_y} + \tan\gamma_y\right)y - r\frac{\tan\gamma_x}{\cos\gamma_y}(1 - \cos\varphi - \tan\varphi\sin\varphi); \quad (20)$$

—the projection of the transitional cutting edge onto plane *xOz*

$$Z_x = \frac{\tan\gamma_x}{\cos\gamma_y}x + (r - \sqrt{r^2 - x^2})\tan\gamma; \quad (21)$$

—the projection of the transitional cutting edge onto plane *yOz*

$$Z_y = \pm\sqrt{r^2 - (y - r)^2}\frac{\tan\gamma_x}{\cos\gamma_y} + \tan\gamma_y \cdot y. \quad (22)$$

The analogous equations for the projections of the previous cutting-edge position (Fig. 4) take the form

$$Z_x = \left(\frac{\tan\gamma_x}{\cos\gamma_y} + \tan\varphi\tan\gamma_y\right)x + \tan\gamma_y[S\tan\varphi + r(1 - \cos\varphi + \tan\varphi\sin\varphi)];$$

$$Z_y = \left(\frac{\tan\gamma_x}{\cos\gamma_y\tan\varphi} + \tan\gamma_y\right)y - \left[\frac{r}{\tan\varphi}(1 - \cos\varphi - \tan\varphi\sin\varphi) + S\right]\frac{\tan\gamma_x}{\cos\gamma_y}; \quad (23)$$

$$Z_x = \frac{\tan\gamma_x}{\cos\gamma_y}x + (r - \sqrt{r^2 - (x + S)^2})\tan\gamma_y;$$

$$Z_y = (\pm\sqrt{2ry - y^2} - S)\frac{\tan\gamma_x}{\tan\gamma_y} + \tan\gamma_y \cdot y.$$

For the given conditions, we plot the lower bounds on the projections of the conditional shear surfaces onto the coordinate planes *AMOB* and the corresponding projections of the preceding cutting-edge position *C'N'M'B* in Fig. 4, on the basis of Eqs. (18)–(23).

Construction of the upper bounds on the conditional shear surfaces *DEB* on the basis of points is based on the formula obtained from triangle *MEN'*:

$$EN' = MN\left(\frac{1}{\tan\varphi_{cu}} + \tan\gamma_d\right), \quad (24)$$

where $MN = a$ is determined from Eq. (24) in [3].

We add the coordinates calculated from Eq. (24) in [3] to the corresponding coordinates of the preceding cutting-edge position. Thus, in Fig. 3, we plot the projections of the conditional shear surfaces F_x and F_y onto the coordinate planes of the machine-tool coordinate system. As for a sharp blade, F_x is constructed by a triangle with base *S*, while F_y has a latent surface adjacent to the curvilinear section of the cutting edge.

The cross section of the chip in its direction of departure is also plotted in Fig. 3. The chip height H_{ch} is determined from the height H_{csp} of the conditional shear surface: $H_{ch} = H_{csp}\cos\gamma_d$.

These examples confirm the validity of the proposed model of chip formation with a single shear surface in constrained oblique cutting by tools with blades of arbitrary shape; this model permits description of the geometry of the chip-forming zone.

Our approach permits the application of solutions obtained for free cutting to constrained cutting; calculation of the shape and dimensions of the chip cross section; and determination of the direction of chip departure over the front surface of the blade.

The chip moves in a certain direction over the tool's front surface at the contact section and then acquires its final shape. It is important to distinguish between the initial direction of chip departure, its motion over the front surface, and the coiling of the chip after its departure from the front surface. We will consider chip transformation in that sequence, on the basis of our model of chip formation with a single conditional shear surface.

It follows from the preceding formulas that the direction of chip departure, specified by the initial departure angle η, is important in investigating the mechanics of constrained metal cutting. To determine η in orthogonal constrained cutting, we resolve the force acting on the cut chip element from the conditional shear surface into components parallel to the *x* and *y* axes (Fig. 5). Obviously, under the action of these forces, the chip will move in the resultant direction within the initial section

$$\tan\eta = P_y^c/P_x^c. \quad (25)$$

Here

$$P_y^c = \int_{F_x}\sigma_{sh}dF_x; \quad (26)$$

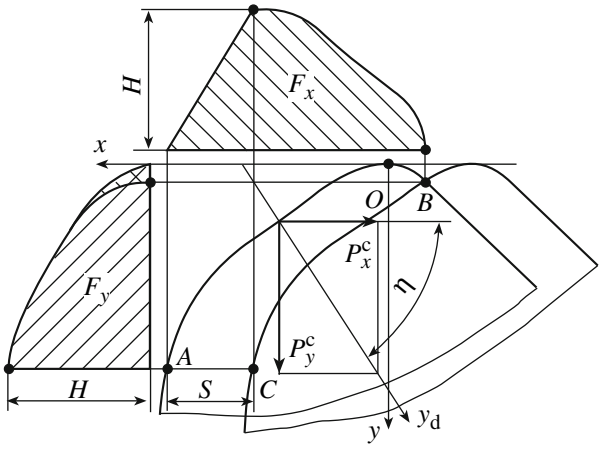

Fig. 5. Determining the initial chip departure angle in orthogonal constrained cutting.

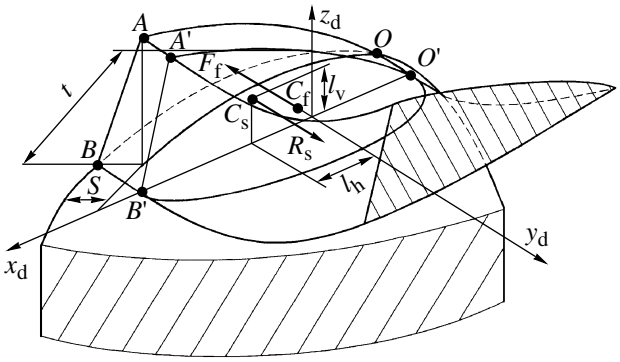

Fig. 6. Coiling of continuous chip.

$$P_x^c = \int_{F_y} \sigma_{sh} dF_y, \quad (27)$$

where σ_{sh} is the stress on the conditional shear surface perpendicular to the z axis.

We assume that the stress distribution along the axis Oz is the same for any point of the cutting edge: $\sigma_{sh} = \sigma_{max} k(z)$, where $k(z)$ is some function depending only on z. Then, substituting this expression into Eqs. (26) and (27) and then into Eq. (25), we find that

$$\tan\eta = F_x/F_y, \quad (28)$$

where F_x and F_y are the areas of the projections of the conditional shear surface onto the planes xOz and yOz (Fig. 5).

Hence, under the given assumptions, determining the initial departure angle of the chip reduces to calculating the areas of the projections of the conditional shear surface onto the coordinate planes. In turn, determining the areas of these projections for specific cases reduces to determining the area of quadrilaterals and curvilinear figures (Figs. 3 and 4).

In oblique constrained cutting, the initial departure angle of the chip will be influenced not only by the ratio F_x/F_y in Eq. (28) but also by the dynamic inclination λ_d of the front surface. Therefore, in this case, Eq. (28) must be rewritten in the form

$$\eta = \arctan(F_x/F_y) \pm \lambda_d. \quad (29)$$

It follows from Eq. (29) that determining the angle of chip departure calls for knowledge of the dynamic inclination of the cutting edge, which depends on η according to Eq. (10) in [3]. It is also evident from Eqs. (11) and (14) that F_x and F_y depend on the chip departure angle. Therefore, numerical solution of Eq. (29) is required, on the basis of successive approximation. The physical explanation here is that the direction of chip departure in constrained cutting is self-stabilizing and adapts to the initial blade geometry and the cutting kinematics by changing the shape and size of the conditional shear surface. An algorithm for calculating η from Eq. (29) was proposed in [7]. Comparison of the calculation results and experimental data reveals satisfactory agreement.

Equation (29) specifies the initial direction of chip direction. Subsequently, chip motion is shifted away from this direction on account of the inclination of the front surface to the basic plane, its curvature, and the plastic deformation of the near-cutter layer. Determining the chip trajectory over the blade's front surface entails taking account of the stress applied to the chip by the conditional shear surface and the contact stress from the front surface. The cutting section of the tool with the root of the chip leaving in direction y_d is shown in Fig. 6 in dynamic conditions: OAB is the conditional shear surface; $O'A'B'$ is the chip cross section. At the contact spot $OO'B'B$ between the chip and the front surface, the normal and tangential stresses are distributed in some definite manner. In the first approximation, we assume that the stress at the conditional shear surface and the frictional stress at the contact spot are uniformly distributed. Then the points of application C_s and C_f of the integral force R_s and R_f will coincide with the centers of gravity of the curvilinear figures $O'A'B'$ and $OO'B'B$. If the chip encounters no obstacles in its path, we set v_c = const and find that $R_s = F_f$. In other words, the forces acting on the chip from the conditional shear surface and the front surface are equal.

In the general case, the coordinates x_d and z_d of points C_s and C_f do not coincide. This gives rise to a bending moment that specifies the natural coiling of the rod [10]. The distance l_v (Fig. 6) determines the torque bending the chip in the vertical plane toward the front surface. At the contact spot, this force is compensated by the nonuniform plastic deformation of the near-cutter layer. After the unloading of the chip at the end of the contact spot, the nonuniformly compressed chip layers undergo elastic recovery, which is observed as upward coiling of the chip from the front surface. The curvature of the coil is determined by the bending moment and the physicomechanical properties of the cut metal.

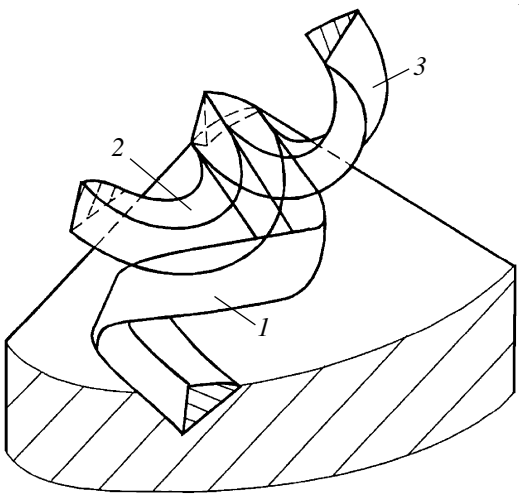

Fig. 7. Types of chip coiling: (*1*) chip of general form; (*2*) plane coiling; (*3*) annular coiling.

The force acting at the distance l_h is responsible for coiling of the chip in the plane of the front surface; this corresponds to the chip trajectory during contact with the front surface. Nonuniform plastic flexure is produced by the nonuniform chip compression. Hence, the ratio of l_h and l_v determines the ratio of the radius and the pitch of the chip spiral.

In oblique cutting, the normal contact stress results in additional shear of the chip. The resultant chip trajectory and its spatial form are determined by the total action of all these factors. If the front surface has a complex topography, as for modern polyhedral cutting plates, the algorithm for trajectory calculation must permit the determination of the normal to the front surface at the location of the chip element at the given time. In this case, we need to describe the motion of the chip as a single body and to establish the boundary beyond which it splits over the width.

Then the chip breaks away from the front surface and undergoes natural coiling. Three possible coiling patterns are shown in Fig. 7. Spiral chip *1* is most common. Annular coiling in the vertical plane (chip *2*) is observed when $l_h = 0$ and the forces P_s and F_f lie in the same vertical plane. Plane coiling (chip *3*) is obtained when the vertical bending moment is completely balanced by the plastic deformation of the near-cutter layer and the elastic recovery of the nonuniformly compressed chip. This provides the basis for the design of chip-breaking systems in the cutting section [14].

Note that chip coiling cannot be fully described on the basis of a single conditional shear surface, since no information can be obtained in that case on the stress in the chip-formation zone and on the shape and dimensions of the contact spot between the chip and the blade's front surface.

REFERENCES

1. Poletika, M.F., *Teoriya obrabotki rezaniem* (Theory of Cutting), Tomsk: Izd. TPI, 1975, vol. 2.
2. Kufarev, G.L., Okenov, K.B., and Govorukhin, V.A., *Struzhkoobrazovanie i kachestvo obrabotannoi poverkhnosti pri nesvobodnom rezanii* (Chip Formation and Surface Quality in Constrained Cutting), Frunze: Mektep, 1970.
3. Petrushin, S.I. and Proskokov, A.V., Theory of Constrained Cutting: Geometry of Constrained Cutting, *Vestn. Mashinostr.*, 2009, no. 11.
4. Zorev, N.N., *Voprosy mekhaniki protsessa rezaniya metallov* (Mechanics of Metal Cutting), Moscow: Mashgiz, 1956.
5. Petrushin, S.I., *Vvedenie v teoriyu nesvodobnogo rezaniya materialov* (Introduction to the Theory of Constrained Cutting), Tomsk: Izd. TPU, 1999.
6. Petrushin, S.I., Bobrovich, I.M., and Korchuganova, M.A., *Optimal'noe proektirovanie formy rezhushchei chasti lezviinykh instrumentov* (Optimal Design of the Cutting Configuration of Tools), Tomsk: Izd. TPU, 1999.